Unsaturated Sulfur Crown Ethers Can Extract Mercury(II) and Show Promise for Future Copernicium(II) Studies: A Combined Experimental and Computational Study

Maryline G. Ferrier[1], Carlos A. Valdez[1,2], Saurabh Kumar Singh[3], Saphon Hok[1,2], Debmalya Ray[4], Laura Gagliardi[5,6] and John D. Despotopulos[1]**

[1] Nuclear and Chemical Sciences Division, Lawrence Livermore National Laboratory, 7000 East Ave., CA 94550, USA

[2] Forensic Science Center, Lawrence Livermore National Laboratory, 7000 East Ave., CA 94550, USA

[3] Department of Chemistry, Indian Institute of Technology Hyderabad, Kandi-502285, Sangareddy, Telangana, India

[4] Department of Chemistry, Chemical Theory Center and Supercomputing Institute, University of Minnesota, Minneapolis, MN 55455, United States

[5] Department of Chemistry, Pritzker School of Molecular Engineering, James Franck Institute, Chicago Center for Theoretical Chemistry, The University of Chicago, 5735 S Ellis Ave, Chicago, IL 60637, United States

[6]Argonne National Laboratory, 97000 S. Cass Ave, Lemont, IL 60439, United States

Keywords: ^{197m}Hg, transactinide, unsaturated thiacrown, extraction, homologs, density functional theory, energy decomposition analysis

Abstract

The unsaturated hexathia-18-crown-6 (UHT18C6) molecule was investigated for the extraction of Hg(II) in HCl and HNO_3 media. This extractant can be directly compared to the recently studied saturated hexathia-18-crown-6 (HT18C6). The default conformation of the sulfur lone pairs in UHT18C6 is endodentate, where the pocket of charge density, according to crystal structures, is oriented towards the center of the ring, which should allow a better extraction for Hg(II) compared to the exodentate HT18C6. Batch study experiments showed that Hg(II) had better extraction at low acid molarity (ca. 99% in HCl and ca. 95% in HNO_3), while almost no extraction was observed above 0.4 M HCl and 4 M HNO_3 (< 5%). Speciation studies were conducted with the goal of delineating a plausible extraction mechanism. Density functional theory calculations including relativistic effects were carried out on both the Hg(II) encapsulated HT18C6 and UHT18C6 complexes to shed light on the binding strength and the nature of bonding. Our calculations offer

insights into the extraction mechanism. In addition to Hg(II), calculations were performed on the hypothetical divalent Cn(II) ion, and results showed that HT18C6 and UHT18C6 could be able to extract Cn(II). Finally, the extraction kinetics were explored to assess if this crown can extract the short-lived Cn(II) species in a future online experiment.

Introduction

Advancing super heavy element (i.e., Z > 104) chemistry is a challenging task due to their scarce production rates and relatively short half-lives (i.e. less than 1 minute for most of them), thus requiring studies to be performed at the atom-at-a-time scale.[1] Because only a single atom is produced, this atom is unable to interact with another atom of the same element and can only interact with its surrounding chemical environment. Computational simulations and theoretical predictions can help with the challenges of experimental studies. Early predictions on the behavior of Cn indicated it may be relativistically stabilized beyond that of its direct-homolog Hg and have interactions more like Rn, due to the spin-orbit splitting of the 6d orbitals resulting in a ground-state configuration with a $6d_{5/2}$ outermost valence orbital. This distinguishes it from the lighter group 12 metals, which have an s outermost orbital.[2] Later calculations indicated that Cn could either form a semiconductor-like solid with clear ability to form chemical bonds,[3] or it should behave like a noble transition metal (similar to other members of group 12 in the periodic table),[4,5] or would have metallic interactions similar to that of its direct-homolog Hg.[6–9] The latest calculations confirmed Pitzer's original hypothesis as to Cn noble-gas-like behavior.[10] Results indicated that Cn exhibits a large band gap of 6.4 eV and is dominated by dispersive interactions, which is largely different from lighter group 12 metals. This behavior was attributed

to the presence of strong scalar relativistic effects and lead to the conclusion that Cn is a relativistic noble liquid significantly more inert than its lighter homologs Hg, Cd and Zn.[10] Recently, successful chemistry experiments were performed on the element 112 (i.e., Cn), however its behavior is still not fully understood. Early gas-phase experiments, which had issues with production and identification methods, indicated that Cn may behave unlike its lighter homolog Hg.[11–13] A more recent gas-phase experiment, which was better optimized,[13] indicated that Cn is a very volatile metal (more so than its homolog Hg) that has a metallic interaction with a gold surface as expected of a typical element of group 12. From these calculations and gas-phase experiments, it is hypothesized that Cn should behave in solution similarly to Hg, albeit being more volatile. As a result, in order to examine possible chemical properties for super heavy elements, the use of homologs such as mercury, Hg(II), is key to developing a suitable extraction system for Cn.

As discussed in our previous work [14], thiacrown molecules are currently under investigation to serve as potential selective and effective extractants of mercury, Hg(II), in nitric and/or hydrochloric acid media. Our previous work involving the saturated thiacrown ether HT18C6 (Figure 1, left) showed that extraction was more efficient in HCl media than HNO_3 media and was completed within minutes for Hg(II). No unique extraction mechanism was deduced from the experiment, which could be attributed to the exodentate configuration of this macrocycle. This configuration could have forced the extracted species to be complexed with multiple thiacrowns configurations and thus leading to slower extraction efficiencies under acidic conditions.[14]

The focus of this study is i) to find a suitable thiacrown-based scaffold extractant that exhibits fast kinetics and high affinity for Hg(II) and ii) to computationally explore the extraction of the

hypothetical divalent Cn(II) ion with HT18C6 and UHT18C6. To suitably compare this exodentate molecule to a similar scaffold having sulfur donor atoms, an endodentate conformation, unsaturated hexathia-18-crown-6 (UHT18C6) has been synthesized (Figure 1, right). As demonstrated by calculations (in this work as well as previously published ones) and crystal structures, the pocket of charge density is oriented toward the center of the macrocyclic ring thus forcing metal coordination to take place within the cavity.[15,16] In the crystalline state, UHT18C6 has six endodentate sulfur atoms, and Hg(II) is shown to sit inside the cavity.[16]

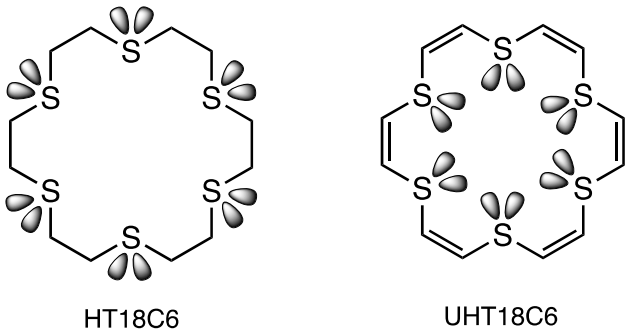

Figure 1. Chemical structures of the saturated and unsaturated hexathia-18-crown-6 ethers, HT18C6 and UHT18C6, showing the orientation of the lone pairs on the sulfur atoms.

Batch experiments were conducted to determine the extraction efficiency of UHT18C6 in carbon tetrachloride (CCl_4) for Hg(II) from a nitric and hydrochloric acid.[14] The extraction kinetics were investigated for Hg(II), and a speciation study was performed to gain insight into the nature of the operating mechanism for the extraction. Herein, we report the experimental work conducted with the aim of establishing a suitable separation scheme for Hg(II) that would give direct insight into the chemical form of the extracted homologs (for Cn) with appropriate kinetics for future

on-line chemistry experiments. Density functional theory calculations including relativistic effects were carried out on both the Hg(II) encapsulated HT18C6 and UHT18C6 complexes to shed light on the binding strength and the nature of bonding. Additionally, calculations were performed on the hypothetical Cn(II) analog to access the geometric and electronic features of (Cn(II):HT18C6/UHT18C6) complexes.

Experimental

Reagents and Materials

Unsaturated hexathia-18-crown-6 (UHT18C6) was synthesized as previously reported [17] and the final purity was determined to be > 98 % confirmed by ^{1}H-NMR ($CDCl_3$). Carbon tetrachloride (CCl_4), sodium thiosulfate pentahydrate ($Na_2S_2O_3 \cdot 5H_2O$) and *cis*-1,2-dichloroethylene were purchased from Sigma-Aldrich (St. Louis, MO.) and used as received. Acids were prepared from ultrapure grade acids and ultrapure water (Seastar) to limit the concentration of impurities such as mercury. The tracer solutions of ^{197m}Hg were prepared with activity concentrations ranging from 2 to 50 cps per 20 µL. The ^{197m}Hg was produced and isolated carrier-free as previously described.[14,18]

Activity Measurements

All activity measurements were performed on a high purity germanium (HPGe) gamma-ray spectrometer coupled with a multi-channel analyzer (DSPEC, Ortec). The detector efficiency was between 0.05% and 11% for the 75-1600 keV range. The spectral line with the highest

relative yield was chosen for determining the activity of ^{197m}Hg (133.99 keV; 33%) and analyzed with Maestro spectral software.

Before each experiment, 0.5 mL of aqueous solution is counted in order to determine the activity of ^{197m}Hg pre-extraction in each tube. Each sample was counted with an HPGe detector for 120 sec (> 1000 counts under the desired photo-peak to obtain the initial activity A_{ini}). After the extraction experiment, 0.3 mL of the aqueous phase (top layer) was removed and placed in a new centrifuge tube containing 0.2 mL acid to maintain the initial counting geometry of 0.5 mL. The aqueous phase samples were counted at the same position and geometry as pre-extraction counts on the same HPGe detector for long enough to obtain sufficient counting statistics (>1000-1600 counts to obtain the aqueous phase activity A_{aq}). Experiments were performed multiple times and all experiments showed excellent reproducibility in trends. The goal of this report is to present data as a qualitative approach to our system to determine if Hg is extracted by the crown ether molecule and if this extraction is performed with fast kinetics. As a result, only one experiment is reported in this report (with the newest ligand batch and the lowest stable Hg impurities present in acids and water) and the errors reported are from propagated counting statistics. During data analysis, all ^{197m}Hg activity measurements were decay corrected. Distribution ratio and percentage of Hg(II) extracted were performed as described in our previous work [14] according to equations (1) and (2):

$$D = \frac{(A_{ini} - A_{aq})}{A_{aq}} \quad (1)$$

$$Percentage\ extracted\ (\%) = \frac{(A_{ini} - A_{aq})}{A_{ini}} \quad (2)$$

Liquid-Liquid Extraction Experiments

The Hg(II) extraction were conducted in HCl and HNO_3 with UHT18C6 dissolved in CCl_4. For batch and kinetics studies, the concentration of crown in CCl_4 was chosen to be the highest concentration possible where UHT18C6 is easily dissolved in CCl_4, which was 1×10^{-4} M.

For the speciation and kinetic studies, the acid concentration was chosen to be 0.4 M HCl or HNO_3. This acid concentration was chosen from batch study results. Experiments were conducted at a concentration where we observed a strong uptake of ^{197m}Hg by UHT18C6, but not at the highest intake observed to avoid high distribution ratio values and thus poor counting statistics due to the low counts from ^{197m}Hg left in aqueous phase.

Batch Experiments

To a 1.5 mL centrifuge tube, 0.48 mL of HCl or HNO_3 ranging in concentration from 0.001 M to concentrated were added. A 20 µL spike containing ^{197m}Hg dissolved in 0.4 M HCl or HNO_3 was added to each centrifuge tube and each tube was gamma counted. The final acid concentration in the vial were 0.017, 0.026, 0.11, 0.21, 0.40, 0.78, 0.98, 1.94, 3.86, 7.70, 9.62, 10.75 M HCl and 0.017, 0.026, 0.11, 0.21, 0.40, 0.78, 0.98, 1.94, 3.86, 7.70, 9.62, 11.54, 14.87 M HNO_3. Using a negative displacement pipet pre-wetted with CCl_4, 0.5 mL of 1×10^{-4} M UHT18C6 dissolved in CCl_4 were added to the centrifuge tube. The solutions were equilibrated for 3 hours on a rotary mixer then placed in a centrifuge for 30 seconds to separate the phases. The aqueous phase was then counted as described above.

To assess if the UHT18C6 was being destroyed by the 3-hour equilibration with acidic solutions, blank batch studies were performed at 0.1 M, 4 M and concentrated HCl and HNO_3. This was done by contacting 0.5 mL of acid with 0.5 mL of CCl_4 containing 1 x 10^{-4} M UHT18C6 for three hours on a vortex mixer. At the conclusion of mixing the aqueous phase was removed and the resulting organic phase containing UHT18C6 was analyzed by gas chromatography – mass spectrometry (GC-MS) to look for any degradation products. No degradation products were found in either HCl or HNO_3 at any acid concentration, indicating that UHT18C6 is resistant to degradation by even concentrated acids (see SI for experimental and GC-MS results).

Speciation Experiments

To a 1.5 mL centrifuge tube, 0.5 mL of ^{197m}Hg dissolved in 0.4 M HCl or HNO_3 were added and gamma counted. Using a negative displacement pipet pre-wetted with CCl_4, 0.5 mL of the desired concentration of UHT18C6 dissolved in CCl_4 were added to the centrifuge tube (i.e., 1×10^{-4} M, 3.2×10^{-5} M, 1×10^{-5} M, 3.2×10^{-6} M, 1×10^{-6} M, 3.2×10^{-7} M and 1×10^{-7} M for the HCl experiment; or 1×10^{-4} M, 5×10^{-5} M, 1×10^{-5} M, 5×10^{-6} M, 1×10^{-6} M, 5×10^{-7} M and 1×10^{-7} M for the HNO_3 experiment). The solutions were mixed on a rotary mixer for about 30 minutes according to the results of the kinetic study, to reach complete equilibrium, then placed in a centrifuge for 30 seconds to separate the phases. The aqueous phase was then counted as described above.

Kinetic Experiments

To a 1.5 mL centrifuge tube, 0.5 mL of ^{197m}Hg dissolved in 0.4 M HCl or HNO_3 were added and gamma counted. Using a negative displacement pipet pre-wetted with CCl_4, 0.5 mL of 1×10^{-4} M of UHT18C6 dissolved in CCl_4 were added to the centrifuge tube. The solutions were mixed on a rotary mixer for the desired time (e.g., 15 sec, 30 sec, 1 min, 5 min, 10 min, 20 min, 1 hour) then placed in a centrifuge for 10 seconds to separate the phases. The aqueous phase was then counted as described above.

Computational Methodology

To understand the Hg(II) encapsulated thiacrowns' geometric and electronic features, density functional theory (DFT) calculations were performed using the ADF-2017 code.[19] All DFT calculations were performed in the scalar relativistic framework, where zeroth-order regular approximation (SR-ZORA) was employed to treat the scalar relativistic effects.[20] Geometry optimizations were performed using the revPEB-D3BJ functional (which includes the Grimme's dispersion correction).[21–25] All these calculations were performed in gas-phase. Slater type all electron TZ2P-type basis sets [26] were used for heavy/super heavy elements Hg, Cn and S atoms, while TZP type basis sets were used for C, H, N, O and Cl of the saturated and unsaturated thiacrown complexes. For calculation of Cn complexes, here we opted for the revPBE functional as Grimme's dispersion interaction for super-heavy elements is not yet implemented in the ADF-2017 code.[27] To make a fair comparison between the Hg(II) and Cn(II), we further computed the Hg structures without Grimme's dispersion (both geometry optimization and single-point energy calculations). Vibrational frequency calculations confirmed the nature of the stationary points as

local minima. All geometry optimizations were performed without any symmetry constraints. Single-point energy calculations were then performed using all-electron TZ2P-type basis sets for all the atoms with a very tight SCF (1×10^{-8} E_h) criterion. The fluxional behavior of thiacrowns results in the formation of multiple low-lying conformers in both free thiacrowns and $HgCl_2$ encapsulated thiacrowns. To predict the possible conformations of $HgCl_2$ encapsulated HT18C6 and UHT18C6 complexes, we performed conformation search analysis using OPLS3 force field parameters [28] as implemented in the Schrödinger suite code. For both the free thiacrown ethers and $HgCl_2$ encapsulated HT18C6 and UHT18C6 complexes, the obtained structures were further optimized using the above-mentioned DFT methods to get more accurate geometric structures and precise energy ordering. In order to study the effect of solvation on the complexation energy of the UHT18C6 and HT18C6 complexes we also performed implicit solvent calculations using the COSMO solvent model and water as solvent for the HgUHT18C6 and HT18C6 complexes.[29,30] Solvent calculations were performed using the revPBE functional with D3BJ dispersion correction.

An energy decomposition analysis (EDA) with an explicit treatment of spin-orbit effects (SO-DFT) as implemented in ADF, was performed to analyze the nature of the interaction and binding energy between the $CnCl_2$ or $HgCl_2$ and the extractant HT18C6 or UHT18C6. To further investigate the impact of spin-orbit effects on the binding energy, we also performed the EDA analysis for the HgUHTC18C6 compound using scalar relativistic DFT (SR-DFT) and compared the SO-DFT values with SR-DFT values (see Table S12 for details). We used all-electron TZ2P basis sets for all atoms with the "nofrozencore" approximation for the EDA calculations. This analysis was performed by decomposing the entire system into two fragments ($HgCl_2$/$CnCl_2$ and

HT18C6/UHT18C6). The binding energy is calculated by performing calculations of the full complex and two fragments.

In EDA, the interaction energy ΔE_{int}, between the fragments was decomposed into individual components, as described in equation (3).

$$\Delta E_{int} = \Delta E_{elec} + \Delta E_{Pauli} + \Delta E_{orb} \quad (3)$$

where ΔE_{elec} and ΔE_{Pauli} denote the attractive electrostatic interaction and the Pauli repulsive energy, respectively, between the fragments. The ΔE_{orb} term describes the stabilizing orbital interaction and includes the electron-pair bonding, charge transfer (HOMO−LUMO interactions), and the polarization term (empty/occupied mixing of orbitals belonging to one fragment due to the presence of the other). Therefore, this orbital component in the decomposition is a measure of the degree of covalency in the interaction.

Results and discussion

Batch Experiments

The effects of HCl and HNO_3 concentration on the uptake of Hg(II) by UHT18C6 in CCl_4 is shown in Figure 2. Consistent with the experiment performed with the saturated hexatia-18-crown-6, HT18C6, strong Hg(II) uptakes are observed at low acid concentrations. At low acid concentration, Hg(II) uptake is about 10 times higher in HCl than in HNO_3. Data showed better extraction in HCl media compared to HNO_3 most likely due to the difference in species sizes, shapes and their ability to interact with the crown.

In HCl, for acid concentrations from ~ 0.001 M to ~ 0.2 M, the distribution ratio is above 100 (extraction > 99%) and dramatically decreases between ~ 0.2 M to ~ 0.8 M to reach a limit of 0.5 at higher acid concentration (extraction < 5%). Due to counting statistic errors associated with the high count rate in the aqueous phase after the extraction study, it was difficult to quantify how much Hg(II) was extracted by UHT18C6 at low acid molarity, which explains the limit set on the lower distribution ratio value (i.e., 0.5).

In the case of the HNO_3 experiment, large uptakes of Hg(II) by UHT18C6 > 95% are observed at low acid concentrations (< 4 M). Similar to the HCl experiments, distribution ratios start to decrease after 0.2 M HNO_3 with a very small decrease at 0.4 M followed by a plateau between ~ 0.4 M and 4 M HNO_3 with an extraction of about 90%. At concentrations above 4 M HNO_3 extractions are extremely low, making counting statistics difficult and thus making us set a limit at a distribution ratio of 0.5 (like for HCl).

One can note that around 0.4 M (where future experiments will be conducted, see Experimental), the D values for HCl are changing rapidly, whereas the D values for HNO_3 are more stable. Therefore, small variations in concentrations which can be attributed to pipetting error (i.e., according to manufacturer specification on the pipette the error on 20 µL is 1.7 µL) could lead to significant differences in the distribution values between batch, speciation, and kinetic studies, but should still be within error.

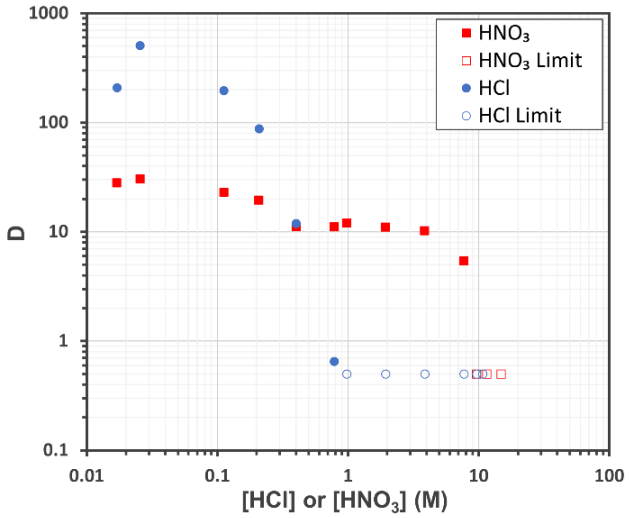

Figure 2. The batch study results showing the distribution ratio (D) of ^{197m}Hg(II) as a function of HNO_3 (0.017M – 14.87 M) and HCl (0.017 M – 10.76 M) with UHT18C6 in CCl_4 with a 3 h equilibration time. Errors are from counting statistics and are contained within the data points.

Speciation Experiments

In theory, plotting the logarithm of the distribution ratios (D) for ^{197m}Hg(II) as a function of the logarithm of the concentration of UHT18C6 should yield a line where the slope of the linear fit corresponds to the number of extractant molecules required to extract each metal atom.[14] If the extraction is consistent and unique, meaning that the same mercury species is extracted by the same molecule configuration, a line is expected in the graph.

In general, only one species of Hg(II) is present in 0.4 M HNO_3, and the speciation study led to a line with a slope of 0.5 in Figure 3. Observing a slope of 0.5 suggests that an equal amount of 1:1 and 2:1 (Hg(II):UHT18C6) complexes are formed. The 1:1 complex supports the notion of Hg(II) being extracted within the cavity of the crown, as observed in crystallographic data.[15,16]

The 2:1 complex could correspond to one crown extracting two Hg(II) molecules, with one sitting slightly above and the other slightly below the cavity. In the section below describing computational results, it has been shown that it is possible to form $Hg(NO_3)_2$:UHT18C6 complexes in the ratio 1:1 and 2:1. The fact that the computational results show that the formation of the 2:1 complex is enthalpically more favorable to form than the 1:1 complex, could explain the 0.4-0.5 slope observed in Figure 3.

As for data measured in HCl, as discussed in our previous work,[14] at 0.4 M HCl, Hg can be present as three distinct species ($HgCl_2$, $HgCl_3^-$ and $HgCl_4^{2-}$) with the latter one being the most prevalent.[14,31–33] First, a linear regression coefficient of 0.74 was found for HCl data which is very low and could not be considered as a good fit. However, when errors were factored into the linear regression, the slope was found to be 0.763 ± 0.142 with a linear regression coefficient of 0.923 does indicate a probable mixture of 2:1 and 1:1 extracted species. From Figure 3, for the HCl data one could note that a possible change can be observed after 1×10^{-5} M, then regressions were performed on two separate regions. From the region 1×10^{-5} to 1×10^{-7} M UHT18C6 the slope was found to be 0.15 ± 0.11 with an R^2 of 0.6319; for the region 1×10^{-4} to 1×10^{-5} M UHT18C6 the slope was found to be 1.88 ± 0.13 with an R^2 of 0.8727. When compared with computation results, we believe that the most likely complexation in HCl is better explained with the redone linear regression factoring uncertainties, , leading to a mixture of 1:1 and 2:1 extracted species.

From the speciation diagram one can see that past 0.1 M HCl, the dominant Hg(II) species in HCl changes from neutral $HgCl_2$ to anionic $HgCl_4^{2-}$. This change of speciation can explain the decrease in Hg(II) extraction with UHT18C6 when the HCl concentration increases, as shown in Figure 2. The batch study shows us that the favored Hg(II) species extracted by UHT18C6 is the

neutral $HgCl_2$ complex. Thus, doing speciation study at 0.4 M HCl can lead to difficult interpretation of the data; multiple species of Hg are present at once and only a small percentage of the Hg (i.e., $HgCl_2$) would be extracted by the thiacrown. No experiments were performed at lower HCl concentration due to lessons learned from previous studies. We have noticed that when ^{197m}Hg is dissolved in low HCl molarity (0.001 – 0.1 M) and in contact with thiacrown dissolved in CCl_4 some discrepancies between distribution ratios calculated from aqueous and organic phases were observed. At low acid molarity, extraction is extremely high and thus distribution ratio values high as well, leading to high activity concentration in the organic phase. Upon removal of all the phases separately, a small discrepancy was observed which could be due to deposition of Hg on the side wall or difficulty to remove all the organic phase due to its viscosity and difficulty to pipette it. Due to experimental difficulty to determine the extraction of Hg(II) at low acid molarity by thiacrowns, we used a computational approach to try to elucidate $HgCl_2$ behavior with thiacrowns such as HT18C6 and UHT18C6.

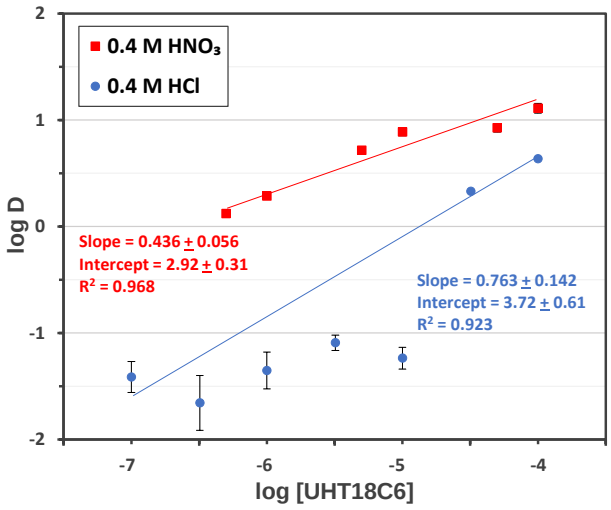

Figure 3. Speciation graph obtained from plotting the logarithm of the distribution ratio (D) of ^{197m}Hg(II) as a function of the logarithm of the concentration of UHT18C6 in CCl_4. Linear trends with their slopes and intercepts and R-squared values are displayed.

Kinetic Experiments

Batch experiments showed that Hg(II) can be extracted by UHT18C6 in CCl_4 in both HCl and HNO_3 after a 3 hour equilibration time. As stated before, Hg(II) is used as a homolog for studying in the future the short-lived isotope of Cn (i.e, ^{285}Cn $t_{1/2}$ = 29 sec). Due to its short half-life and the fact that chemistry will have to be performed at the atom-at-a-time scale, an online chemical separation will have to be conducted. This type of extraction requires kinetics to be in the order of seconds versus hours. The kinetics of the uptake of Hg(II) by UHT18C6 at 0.4 M HCl and HNO_3 were examined (see Figure 4). One can note from the batch study experiment (Figure 2) that even if the distribution ratio in HCl decreases between 0.2 M and 1 M HCl, the D value at 0.4 M HCl and 0.4 M HNO_3 are similar. According to Figure 4, full equilibrium was reached within 5 minutes. After 15 seconds, Hg(II) is being extracted by UHT18C6 from both HCl and HNO_3 matrices, with a higher uptake in HNO_3. After 30 seconds, extraction in HNO_3 was near 100% while in HCl only 20% Hg(II) was extracted by UHT18C6. The extraction reached 80% after 3 minutes in HCl. The extraction in HCl is probably not fast enough for a Cn experiment, although it could be achieved in HNO_3. The extraction seems to be faster in HNO_3 than in HCl, which might be due to the difference of the counter ions involved in the processes. Mercury nitrate is considered a strong electrolyte whereas mercury halide a very weak one. The difference in the covalent bond character between Hg(II) and Cl^- and NO_3^- can be interpreted

from the pH value at which HgO precipitates. It shows well that mercury chloride is more covalent than mercury nitrate, and thus less likely to dissociate.[34] These modes of coordination by the different counterions could potentially give enough freedom to the mercury nitrate species to bind to the available sulfur lone pairs in the crown. Another striking difference between the two media is the fact that only 1 species exist in HNO_3 while multiple species coexist in HCl. Performing extraction at lower acid molarity could result in higher extraction percentage in HCl since $HgCl_2$ species would be dominant in solution.

Performing extraction with a better mixing system consisting of small contactors will allow consistent and adequate phase mixing. Additionally, performing the experiment at lower acid concentrations should yield similar kinetics with stronger uptakes at shorter times, according to batch study results. Thus, favorable conditions could be obtained, after optimization, to proceed to online experiments with Cn.

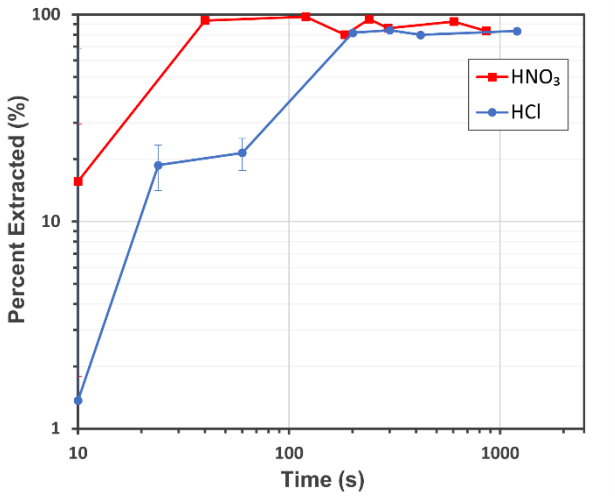

Figure 4. Kinetics uptake of $^{197m}Hg(II)$ in 0.4 M HNO_3 and HCl media with UHT18C6 dissolved in CCl_4 (10^{-4} M) at varying equilibration times. Errors are from counting errors and if not observed they are contained within the data points.

Computational Results

First, the structural aspects of free saturated (HT18C6) and unsaturated (UHT18C6) thiacrowns were analyzed. Approximately 30 of the lowest energy conformers were further optimized using density functional theory (DFT) methods (see computational methods for geometry optimization) to get precise energy ordering of the structures. Nineteen different low-lying DFT optimized structures for both the UHT18C6 and HT18C6 within the energy range of ~ 5 kcal/mol are reported (see ESI, Table S1-S2). From the DFT optimized geometry and energetics, it is evident that free saturated thiacrowns have a significant degree of flexibility compared to the unsaturated thiacrown structures (see Table S1-S2). The optimized geometry of all these conformers is provided in the ESI (Table S8-S9). This behavior is rooted back to the presence of the double bonds in the unsaturated thiacrown, which hinders the C-C bond rotations resulting in fewer conformers. To obtain the minimum energy structure for $HgCl_2$ encapsulated thiacrowns, we first performed the conformational analysis on both HT18C6 and UHT18C6. Conformational analysis on $HgCl_2$ encapsulated HT18C6 shows the formation of multiple low-lying conformers within the range of ~5 kcal/mol. The observed ground state configuration has no symmetry, and belongs to the C_1 point group, where $HgCl_2$ coordinated with three –S atoms from the HT18C6 (see Figure 5 right). The DFT optimized structure is in close resemblance with the previously reported crystal structure.[16] Out of the studied conformers (see Table S6), several low-lying

conformers were observed within ~1 kcal/mol range of energy, where $HgCl_2$ binds similarly to other –S atoms of HT18C6. This suggests the high-flexibility nature of HT18C6 in binding with $HgCl_2$. This geometric arrangement (open site at Hg center) opens up the possibility of coordinating with –S atoms of another HT18C6 to form a typical octahedral geometry around Hg(II) (vide infra). In contrast to HT18C6, $HgCl_2$ shows preference in binding with UHT18C6, as we noticed the formation of one thermodynamically stable structure compared to other possible conformers (see Table S4-S5). The lowest-energy DFT optimized structure of $HgCl_2$ encapsulated UHT18C6 shows endodentate arrangement of unsaturated thiacrowns, where Hg(II) resides in an eight-coordinated hexagonal bipyramidal environment. The six –S atoms reside in a hexagonal plane, while both –Cl atoms occupy the axial position. The calculated average (avg.) Hg-S bond length is ~3.302 Å, and the avg. Hg-Cl bond length is ~2.367 Å, and these values are in good agreement with the experimental structure (3.193 Å /2.312 Å for avg. Hg-S / avg. Hg-Cl bond length, respectively).[16] The DFT optimized geometry of $HgCl_2$ encapsulated UHT18C6 is shown in Figure 5, left. The other possible conformers are significantly higher in energy >5 kcal/mol (Table S4 and S7). Conformational analysis and DFT optimization suggest that both HT18C6 and UHT18C6 show a strong affinity towards $HgCl_2$ binding; however, the latter prefers to form a stable eight-coordinated complex. Our structural analysis indicates that the UHT18C6 ligand framework offers a high selectivity towards encapsulation of $HgCl_2$. This would most likely explain why the kinetics of Hg(II) extraction is faster with UHT18C6, described in this work, compared to HT18C6.[14]

To further understand the free energy of complexation for both $HgCl_2$ encapsulated HT18C6 and UHT18C6, we have computed the average ΔG value by thermal averaging the Gibbs free energy

of the low-lying conformers. The following equations have been used to estimate the average ΔG:

$$\Delta G = G_{complex} - (G_{Crown}) - G_{HgCl2} \quad (4)$$

$$\Delta G_{avg} = G_{min} - (RTln(\sum exp^{\frac{-Gi}{RT}}) \text{ (where i = each of the studied structures)} \quad (5)$$

$$\Delta G_{avg} = G_{avgComplex} - (G_{avgCrown}) - G_{HgCl2} \quad (6)$$

where ΔG is the Gibbs free energy of complexation. Due to multiple low-lying structures, we have calculated the Gibbs free energy for several conformers. The Gibbs free energy was calculated for all the conformers of HT18C6, UHT18C6 lying within the energy range of 5 kcal/mol from the lowest one and their complexes with $HgCl_2$ (see Table S1-S4). The structure with the largest G value is considered G_{min}, and then we have calculated the thermal averaging of Gibbs free energy of the low-lying structures (using equation 5). The thermal averaging has been performed for both free HT18C6/UHT18C6 crown ethers (represented by $G_{avgCrown}$) and $HgCl_2$ encapsulated HT18C6/UHT18C6 (represented by $G_{avgComplex}$). The DFT calculated Gibbs free energies and enthalpies are provided in Table S1-S4 for all the conformers. The calculated average free energy of complexation with dispersion interaction is -8.4 kcal/mol and -11.4 kcal/mol for the $HgCl_2$:UHT18C6 complexes and $HgCl_2$:HT18C6 complexes, respectively (see Table 1). From the energetic perspective, it is obvious that the HT18C6 complex shows a stronger affinity for the complexation than the UHT18C6 complex. Moreover, the role of the solvent on the complexation energies for both the $HgCl_2$:HT18C6 and $HgCl_2$:UHT18C6 complexes have been tested. Calculations on the lowest energy conformers revealed that the incorporation of solvent further increases the complexation energy by 3-5 kcal/mol (see Table

S11), thus the solvent is expected to play an important role in determining the trends in the complexation energy. The presence of numerous low-lying conformers (≤ 1 kcal/mol) for $HgCl_2$:HT18C6 adds a hefty contribution to its free energy, resulting in a significantly large free energy of complexation for HT18C6 thiacrowns. However, it is important to note here that HT18C6 also has a similar number of low-lying conformers, thus, the conformational entropic penalty upon complexation is expected to be marginal, resulting in a minimal change in the complexation energy (see Table S13). On the other hand, due to the formation of a stable eight coordinated $HgCl_2$:UHT18C6 complex, the effect of conformational entropy is much higher on the complexation energy compared to the $HgCl_2$:HT18C6 complex. Although we noticed that the UTH18C6 thiacrown prefers a selective binding with $HgCl_2$, the presence of numerous low-lying conformers for HT18C6 thiacrown results in a strong affinity for the $HgCl_2$ extraction. This would directly affect the extraction mechanism as HT18C6 favors the formation of multiple complexes, while UHT18C6 is highly selective as it preferably forms an eight-coordinate hexagonal bipyramidal geometry. In addition to the fact that Hg(II) has multiple species between 0.1 M and 1 M HCl, and would thus complicate the interpretation of the extraction mechanism, the formation of multiple complexes between $HgCl_2$ and HT18C6 would explain why in our previous work we were not able to determine an unique extraction mechanism during our speciation study.[14] The computational results presented here show that only one conformation of $HgCl_2$ and UHT18C6 is stable (see Figure 5, left). This suggests that the difficulty of interpreting the speciation between Hg(II) and UHT18C6 in HCl is mainly due to the presence of multiple Hg species. We also checked the effect of basis set superposition error (BSSE) for the 1:1 $HgCl_2$:UHT18C6 complex and found the overall change in complexation energy due to BSSE

correction (see SI section on BSSE) is only -1.5 kcal/mol which is much smaller than the overall complexation energy and hence will not affect results significantly.

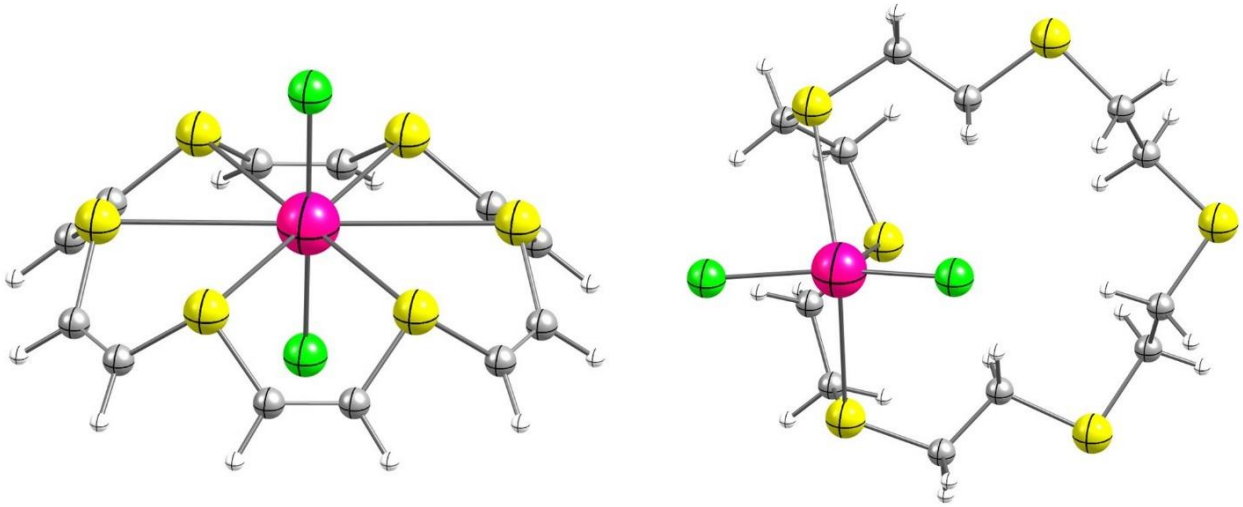

Figure 5. DFT optimized geometry of the most stable conformer of [Hg^{II}(18-UHT18C6)Cl_2] (left); and the low-lying structure for [Hg^{II}(18-HT18C6)Cl_2] (right). Color Code: Pink (Hg), Yellow (S), light green (Cl), grey(C), and white (H).

To further understand the strength of the binding, we performed an EDA analysis at the DFT optimized geometry of $HgCl_2$ encapsulated HT18C6 and UHT18C6, using spin-orbit relativistic methods (SO-DFT). Table 1 summarizes the different contributions to the binding energy for both complexes. The total binding energy for the HT18C6 complex is ~ 6.4 kcal/mol higher than the one for the UHT18C6 complex (Table 1), and this is in agreement with the trend observed for the free energy of complexation suggesting that the HT18C6 complex will be a better extractant for Hg(II) considering the thermodynamic factor only. The orbital interaction in the HT18C6

complex is ~2 times larger than in the UHT18C6 complex. Such a large difference (~ 60 kcal/mol) between the HT18C6 and UHT18C6 is related to the difference in the structural parameters, where the first one has a shorter Hg-S bond length (3.017 Å) compared to UTH18C6 (~3.302 Å). The shorter Hg-S bond in HT18C6 results in a substantial overlap between the 6s orbital of Hg(II) and 3p orbitals of HT18C6 compared to UHT18C6. The difference of the avg Hg-S bond length is also reflected in the computed electrostatic energy, which is slightly larger for HT18C6 than UTH18C6. On the other hand, the Pauli term contains the exchange and repulsion energies and this value is more stabilizing for the UHT18C6 complex. This stabilization is due to the formation of a rigid framework around the Hg(II) ion, i.e. an eight-coordinated hexagonal bipyramidal environment, where all the -S atoms are placed in the hexagonal plane. This results in a dramatic decrease in the Pauli repulsion for UTH18C6, which favors UTH18C6 compared to HT18C6 (see Table 1). The computed dispersion interaction energy is ~ 5 kcal/mol higher for the UHT18C6 complex compared to the HT18C6 complex. Although the dispersion and the Pauli repulsion are favorable for UTH18C6, a relatively stronger orbital and electrostatic interaction makes the binding stronger for the HT18C6.

Table 1. Energy decomposition analysis for complex $HgCl_2$ with both UHT18C6 and HT18C6 complexes using spin-orbit relativistic methods. All these values are reported in kcal/mol.

Parameters	**UHT18C6**	**HT18C6**

Pauli Repulsion	97.8	163.9
Electrostatic	-43.4	-60.6
Orbital Interaction	-54.4	-114.4
Dispersion	-27.2	-22.5
Total Binding Energy	**-27.2**	**-33.6**
% of covalency	55.6	65.4
Enthalpy of Complexation	-19.9	-22.7
Free Energy of Complexation	-8.4	-11.4

Binding energy was calculated by computing $HgCl_2$, and thiacrown separately

Sevdic´ and co-workers reported that the complexation of 18-membered saturated thiacrown ether, 1,4,7,10,13,16-hexathiacyclooctadecane (18S6, called HT18C6 in this work), with 1 and 2 equivalent of $HgCl_2$ afforded 1:1 and 1:2 macrocycle/metal complexes, respectively.[35,36] In another report, Tsuchiya and co-workers reported the formation of a linear chain structure.[16] These results suggest that numerous structures are possible with varying ratios of $HgCl_2$ and the macrocycle. To further investigate the complexation using the HT18C6 species and its impact on the extraction, we designed some model complexes with a 1:2 and 2:1 ratio of $HgCl_2$ and HT18C6 thiacrown. The model with a 1:2 ratio of $HgCl_2$ and HT18C6, mimics the possibility of forming polymeric linear chain structures.[16] DFT optimization predicts an octahedral environment around Hg(II) ion, where four -S atoms are in the basal plane (two from each

macrocycle) and two -Cl atoms occupy the axial position (see Figure 6, left). The average Hg-Cl and Hg-S bonds are 2.567 Å and 2.865 Å and respectively, in good agreement with experimental structures (2.670 Å and 2.716 Å for avg Hg-Cl and avg. Hg-S bonds). The calculated average free energy for complexation is -10 kcal/mol for a 1:2 ratio of $HgCl_2$ and HT18C6.

The second model with a 2:1 ratio of $HgCl_2$ and HT18C6 results in a complex where one macrocycle binds the two $HgCl_2$. This arrangement is reported earlier by Herceg et al., where two $HgBr_2$ units are attached to HT18C6 in a –trans fashion.[37] DFT optimization of 2:1 $HgCl_2$:HT18C6 complex results in a structural topology that is very similar to the crystal structure of 2:1 $HgBr_2$: HT18C6 complex.[37] The computed avg. Hg-S and avg. Hg-Cl bond lengths are 2.886 Å and 2.401 Å, respectively. The structural arrangement resembles the optimized structure obtained for the 1:1 ratio (see Figure 6, right). The calculated average free energy complexation for the 2:1 ratio of $HgCl_2$ and HT18C6 is -13 kcal/mol. This is similar to the value obtained for the 1:1 ratio of free energy of complexation (-11.4 kcal/mol). Overall, the formation of multiple low-lying conformers and the possible formation of several polymeric chain structures 1:2 and 2:1 Hg/HT18C6 ratio makes HT18C6 very efficient for extracting $HgCl_2$.

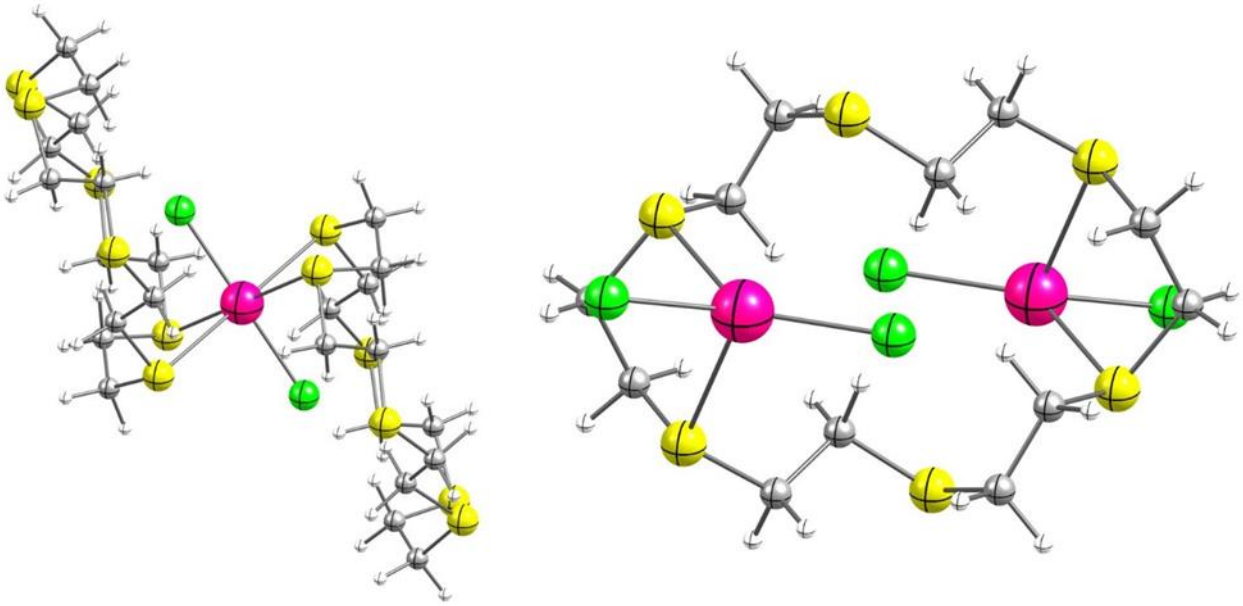

Figure 6. DFT optimized geometry of polymeric structures with 1:2 (left) and 2:1 (right) ratio of $HgCl_2$ and HT18C6 thiacrown complexes. Color Code: Pink (Hg), Yellow (S), light green (Cl), grey(C), and white (H).

On the other hand, concerning UHT18C6, Hg(II) is isolated in a very stable eight-coordinate hexagonal bipyramidal arrangement due to the molecule rigidity. Since there is no experimental evidence for polymeric/chain structures, we have restricted our studies to the 1:1 (*vide supra*) and 2:1 ratios of $HgCl_2$ and UHT18C6. The DFT optimized geometry for the 2:1 complex suggests that one $HgCl_2$ unit is sitting slightly above and the other one slightly below the cavity of UHT18C6. The calculated avg. Hg-S bond distance is ~ 3.125 Å, which is longer than the avg. Hg-S bond length observed for a similar model complex with HT18C6 (2.886 Å). The calculated free energy of complexation is found to be +2.1 kcal/mol (compared to the -8.4 kcal/mol of the 1:1 UHT18C6 complex). However, the computed enthalpy for the complexation is -18.5 kcal/mol, which is very similar to the enthalpy of complexation obtained for 1:1 ratio (-20

kcal/mol). Thus, the complexation of both 1:1 and 1:2 ratios of $HgCl_2$ and UHT18C6 is an enthalpically driven process. It should be noted that for the 2:1 $HgCl_2$:UHT18C6 complex, the entropy factor is penalizing the free energy more than that in the 1:1 $HgCl_2$:UHT18C6 complex, making the free energy slightly positive. In summary, the extraction mechanism of UHT18C6 has mainly been driven by the formation of a stable 1:1 Hg:UHT18C6 eight-coordinated hexagonal bipyramidal complex, followed by other possible conformers, but the formation of 2:1 ratio and other possible conformations cannot be ruled out.

We also performed DFT calculations for the 1:1 and 2:1 $Hg(NO_3)_2$:UHT18C6 complexes. Our study shows that the free energy of formation of 1:1 and 2:1 complexes are -18.3 and -10.1 kcal/mol, respectively, whereas the enthalpy of formation are -28.8 and -33.6 kcal/mol, respectively (see Table S10). Similar to the $HgCl_2$:UHT18C6 complex in 1:1 and 2:1 ratio, here also we see that the free energy of formation for the 1:1 complex is more negative than that of the 2:1 complex, but here, the enthalpy of formation of 2:1 complex is more negative than that of the 1:1 complex. This again suggests that both the 1:1 and 2:1 complexes are favorable to form, confirming the observation of a slope of ca. 0.5 in the speciation study.

Additionally, we performed calculations on the super-heavy element Cn(II) to understand the structural and electronic properties of the Cn(II):HT18C6/UHT18C6 complexes and compare them to the Hg(II) analog. The goal is to explore if these molecules could eventually be used to extract Cn(II). We optimized both the 1:1 Cn(II): HT18C6/UHT18C6 ratio complexes along with two other possible structures with 1:2 and 2:1 Cn(II):HT18C6 ratios. The 1:1 geometry of Cn(II):HT18C6/UHT18C6 is similar to the one of the Hg(II) species. The optimized structure of Cn(II):UHT18C6 shows that the averages Cn-S and Cn-Cl distances of ~3.444 Å and ~2.377Å, respectively, are marginally higher than their Hg(II) analogs. The obtained trend is in line with

the previous studies on divalent Cn complexes.[38] EDA analysis was performed further to understand the strength of the binding (see Table 2). Calculations were performed with revPBE functionals without dispersion interaction for Cn(II) and Hg(II) analogs (as the dispersion correction is not available for superheavy element Cn) for comparison (see Table S10). Table 2 offers a detailed comparative analysis of the binding energy and its decomposition for the Cn and Hg in both HT18C6 and UHT18C6 thiacrowns. From Table 2, it is evident that the HT18C6 complex has a stronger affinity for $HgCl_2$ than the UHT18C6. On the other hand, we noticed a dramatic decrease in Cn's binding energy with the HT18C6 complex, where the binding energy is found to be ~2.51 kcal/mol. The smaller single-bond covalent radii of Cn (1.22 Å) than the Hg (1.33 Å), followed by the relativistic contraction of the valence orbitals (spinors), might be the cause for the weaker orbital overlap. The reduction in orbital interaction energy decreases the Cn(II):HT18C6 complex's binding energy compared to the Hg(II) analog. Contrarily, the orbital interactions are much favored for the Cn:UHT18C6 complex, however the presence of significant Pauli repulsion disfavors the formation of the Cn:UHT18C6 complex. A similar binding energy preference is observed for the 1:2 and 2:1 Cn:HT18C6 complexes (see Table 3). Similar to the HT18C6 complexes, we also noticed a significant decrease in binding energy for the $CnCl_2$:UHT18C6 complex compared to the analogous $HgCl_2$:UHT18C6 complex. In fact, the binding energy for the $CnCl_2$:UHT18C6 complex is positive, suggesting that the complexation is not feasible. However, we would like to point out that these interaction energies for Cn complexes are without dispersion correction. As shown in Table 1 and Table 2, the interaction energy for the $HgCl_2$:HT18C6/UHT18C6 becomes ~25 kcal/mol more negative when dispersion corrections are included in our calculations. Similar to the interaction energy, we also noticed that without dispersion correction, the free energy and enthalpy of formation of Hg complexes

are also more positive (see Table 2). Thus, we believe that the interaction energy, free energy and enthalpy of the Cn complexes can also be negative if dispersion could be included in the calculations (both for the geometry optimization and single-point energy calculation), and hence, the Cn complexes can in principle be extracted using thiacrowns.

Table 2. Energy decomposition analysis for the complex $HgCl_2$ (and $CnCl_2$ in parentheses) with both UHT18C6 and HT18C6 complexes using spin-orbit relativistic methods. All values are in kcal/mol. All the calculations were performed with revPBE without dispersion correction.

Parameters	**UHT18C6**	**HT18C6**
Pauli Repulsion	84.0 (67.2)	71.4(11.6)
Electrostatic	-36.6 (-29.5)	-24.7 (-2.8)
Orbital Interaction	-48.8 (-30.3)	-57.1 (-11.3)
Total Binding Energy	**-1.4 (7.4)**	**-10.3 (-2.5)**
% of covalency	57.1(50.7)	69.7(80.1)
Enthalpy of Complexation	3.2 (13.3)	-5.8(-2.7)
Free Energy of Complexation	12.4 (24.6)	6.9(11.7)

Binding energy was calculated by fragmenting molecule in MCl_2 (M = Hg and Cn) and UHT18C6 and HT18C6

Table 3. Energy decomposition analysis for complex $CnCl_2$ with HT18C6 complexes in 1:2 and 2:1 ratio using spin-orbit relativistic methods. Free energy and enthalpy of formation of $CnCl_2$ and HT18C6 complexes are also reported. All values are in kcal/mol. All the calculations were performed with revPBE without dispersion correction.

Parameters	**2:1 $CnCl_2$:HT18C6**	**1:2 $CnCl_2$:HT18C6**
Pauli Repulsion	13.4	13.3
Electrostatic	-3.1	-3.3
Orbital Interaction	-14.5	-13.6
Total Binding Energy	**-4.1**	**-3.6**
% of covalency	82.4	80.6
Enthalpy of Complexation	-3.4	-7.5
Free Energy of Complexation	30.9	30.1

Binding energy was calculated by fragmenting molecule in $CnCl_2$ and HT18C6

Conclusions

Thiacrown ethers have been studied for mercury extraction in HCl and HNO_3. This study of unsaturated hexathia-18-crown-6 (UHT18C6), in conjunction with the previous study with the

saturated molecule (HT18C6)[14], was pursued in order to develop a suitable chemical extracting system for Hg(II) using non-carrier added mercury ^{197m}Hg.

Batch experiments determined a high extraction efficiency at low acid molarity for both extractants. Concerning the UHT18C6 experiments presented in this paper, it was demonstrated that the extraction was more efficient in HCl media at low molarity with a high extraction (> 99%) and distribution ratio. With increasing acid molarity the extraction efficiency decreased to almost none above 0.4 M HCl, which could be explained by the change of Hg(II) speciation in HCl going from $HgCl_2$ at low molarity and changing to a mixture of comparable concentration of the species $HgCl_2$, $HgCl_3^-$ and $HgCl_4^{2-}$ between 0.1 and 1 M, and to having a majority of $HgCl_4^{2-}$ species present above 1 M HCl. On the other hand, in HNO_3 media, distribution ratio changed significantly only after 4 M HNO_3.

When comparing both extractants, their conformation difference (exodentate for HT18C6 vs. endodentate UHT18C6) have the potential to have different extraction mechanisms, as demonstrated from computational studies. We learned that it was extremely difficult to determine extraction speciation experimentally due the presence of multiple species for Hg in HCl and also the possibility of having multiple conformers for the extractant molecules HT18C6 and UHT18C6 as demonstrated by DFT calculations. Calculations yielded the formation of numerous low-lying conformers within the $\leq$ 1kcal/mol for 1:1 ratio along with the possibility of forming 1:2 and 2:1 (Hg(II):HT18C6) complexes. On the other hand, DFT calculations yield the formation of stable 1:1 species for Hg(II) being extracted into the cavity of UTH18C6. Alongside, we have observed the formation of 2:1 (Hg(II):HT18C6) and Hg(II):UHT18C6 where one crown extracting two Hg(II) molecules, with one sitting slightly above and the other slightly

below the cavity is possible when we look at the enthalpy results. Our comparative analysis suggests both the HT18C6 and UHT18C6 are the potential extractant for Hg(II).

Batch studies and computational data showed that it was possible to extract Hg(II) using UHT18C6 in HCl and HNO_3. Extraction kinetics are of high importance to assess to experiment feasibility with Cn. The extraction of Hg(II) was performed within minutes (after 30 seconds, extraction in HNO_3 was near 100% while in HCl only 20% Hg(II) was extracted by UHT18C6), This demonstrates that the use of sulfur in an endodentate configuration in the crown ether molecule was effective to increase the affinity, selectivity and kinetics with respect to Hg(II). As shown by the calculations, UHT18C6 has a more restrained conformation and thus less coordination geometries available when compared to HT18C6, and thus their kinetics are most likely to show significant differences.

DFT calculations show that sulfur in the crown ether (both the UHT18C6 and HT18C6) is very promising towards the extraction of Hg(II). In particular, the performance of HT18C6 is much more efficient compared to UHT18C6 due to the formation of multiple low-lying conformers within ≤ 1 kcal/mol. The asymmetric ground state configuration of Hg(II): HT18C6 is favored by the Pauli repulsion, making HT18C6 a slightly better extractant than UTH18C6. These static DFT calculations are purely thermodynamical and show that the HT18C6 complex is favorably formed, even if HT18C6 has multiple low-lying conformations while UHT18C6 has a single rigid low lying conformation. DFT calculations suggest that the Cn complexes with HT18C6 and UHT18C6 show relatively weaker binding energy than the Hg(II) analog. The EDA analysis suggests that a weaker orbital interaction resulting from relativistic contraction of the orbitals and smaller covalent radii might be the cause for the decrease in the binding energy. The calculations show that HT18C6 can extract the Cn(II) analog. The UHT18C6 conformation may

also be able to extract the Cn(II) analog, but this cannot be confirmed due to unavailability of dispersion corrections for calculations involving the Cn atom.

Our studies demonstrated the attraction to use endodentate conformation thiacrowns, in order to increase the affinity with Hg(II). Future work will focus on the potential synthesis of new thiacrown derivatives with substituents attached to the ring. The substituents can play different roles in the extraction 1) it can force the endodentate configuration (i.e., sulfur lone pair oriented towards the cavity of the crown) and 2) it could allow the incorporation of a pendant arm that would allow attachment to a solid support in order to study chromatographic extraction compared to liquid-liquid extraction.[39] The new macrocycle should allow for a fast kinetic and high affinity for Hg(II). From the comparison of Hg(II) extraction data with future data obtained with Cn with the same molecule will allow to extrapolation of the transactinides behavior, allowing determination of any Hg-like properties.

ASSOCIATED CONTENT

Supporting Information. All available data are included in the supporting information (SI) and is available free of charge. The SI contains 1) Analysis of the stability of the unsaturated thiacrown ether in HCl and HNO_3 organic extracts, and 2) Computational supplemental details containing: a) tables for DFT optimized low-lying conformers along with the absolute SCF electronic energy, enthalpy (H) and Gibbs free energy (G) for free UHT18C6, free HT18C6, $HgCl_2$:HT18C6, and $HgCl_2$:UHT18C6; b) tables for DFT optimized geometry of Hg and Cn complexes with both HT18C6 and UHT18C6; c) tables for DFT optimized structure of low-lying conformers for $HgCl_2$:HT18C6, $HgCl_2$:UHT18C6 complexes, HT18C6 and UHT18C6; d) table for absolute SCF electronic energy, enthalpy (H) and Gibbs free energy (G) for various Hg(II) and Cn(II) complexes using DFT; e) Gibbs free energy (kcal/mol) of complexation of $HgCl_2$:UHT18C6 and

$HgCl_2$:HT18C6 in gas phase and solvent phase (water) using revPBED3BJ functional; f) Energy decomposition analysis for complex $HgCl_2$ with UHT18C6 complex using spin-orbit relativistic and scalar relativistic methods; g) DFT computed Gibbs free energy of the lowest conformer and contributions emerging from the low-lying conformers and h) details about BSSE Correction..

AUTHOR INFORMATION

Corresponding Author

John Despotopulos. Nuclear and Chemical Sciences Division, Lawrence Livermore National Laboratory. 7000 East Ave, Livermore, CA 94550, United States orcid.org/0000-0002-2350-5103; E-mail: despotopulos1@llnl.gov.

Laura Gagliardi. Department of Chemistry, The University of Chicago. 5735 S. Ellis Ave, Chicago, IL 60637, United States; E-mail: lgagliardi@uchicago.edu.

Authors:

Maryline G. Ferrier - Nuclear and Chemical Sciences Division, Lawrence Livermore National Laboratory, 7000 East Ave., CA 94550, United States; orcid.org/0000-0003-0081-279X

Carlos A. Valdez - Nuclear and Chemical Sciences Division and Forensic Science Center, Lawrence Livermore National Laboratory, 7000 East Ave., CA 94550, United States; orcid.org/0000-0002-8641-9077

Saurabh Kumar Singh - Department of Chemistry, Indian Institute of Technology Hyderabad, Kandi-502285, Sangareddy, Telangana, India; orcid.org/0000-0001-9488-8036

Saphon Hok - Nuclear and Chemical Sciences Division and Forensic Science Center, Lawrence Livermore National Laboratory, 7000 East Ave., CA 94550, United States

Debmalya Ray - Department of Chemistry, Chemical Theory Center and Supercomputing Institute, University of Minnesota, Minneapolis, MN 55455, United States

Author Contributions

The manuscript was written through contributions of all authors. All authors have given approval to the final version of the manuscript.

Note: The authors declare no competing financial interest.

ACKNOWLEDGMENT

This study was performed under the auspices of the U.S. Department of Energy by Lawrence Livermore National Laboratory under Contract DE-AC52-07NA27344. This work was funded by the Laboratory and Development Program at LLNL under project tracking code 19-ERD-003. This material is based upon work supported by the Department of Energy National Nuclear Security Administration through the Nuclear Science and Security Consortium under Award Number DE-NA0003180. The computational part of this work was funded by the Division of Chemical Sciences, Geosciences, and Biosciences, Office of Basic Energy Sciences of the U.S. Department of Energy through Grant DE-SC002183 (LG and DR). SKS acknowledges the Department of Science and Technology for the Start-up Research Grant (SRG/2020/001323) and IIT Hyderabad for generous funding. The authors would like to thank the CAMS facility staff at LLNL, specifically Scott Tumey, Thomas Brown and Grahm Bench for providing beam time and

expertise to the production of radionuclides used in this study. The calculations were performed at the Minnesota Supercomputing Institute. [LLNL-JRNL-823071]

ABBREVIATIONS

UHT18C6, unsaturated hexathia-18-crown-6; HT18C6, saturated hexathia-18-crown-6; HNO_3, nitric acid; HCl, hydrochloric acid; CCl_4, carbon tetrachloride; HPGe, high purity germanium; DFT, density functional theory; zeroth-order regular approximation (SR-ZORA); EDA, energy decomposition analysis; EI-GC-MS (electron ionization gas chromatography-mass spectrometry).

REFERENCES

(1) Schädel, M. Chemistry of the Superheavy Elements. *Philos. Trans. R. Soc. Math. Phys. Eng. Sci.* **2015**, *373* (2037), 20140191. https://doi.org/10.1098/rsta.2014.0191.

(2) Pitzer, K. S. Are Elements 112, 114, and 118 Relatively Inert Gases? *J. Chem. Phys.* **1975**, *63* (2), 1032–1033. https://doi.org/10.1063/1.431398.

(3) Gaston, N.; Opahle, I.; Gäggeler, H. W.; Schwerdtfeger, P. Is Eka-Mercury (Element 112) a Group 12 Metal? *Angew. Chem. Int. Ed.* **2007**, *46* (10), 1663–1666. https://doi.org/10.1002/anie.200604262.

(4) Eliav, E.; Kaldor, U.; Ishikawa, Y. Transition Energies of Mercury and Ekamercury (Element 112) by the Relativistic Coupled-Cluster Method. *Phys. Rev. A* **1995**, *52* (4), 2765–2769. https://doi.org/10.1103/PhysRevA.52.2765.

(5) Seth, M.; Schwerdtfeger, P.; Dolg, M. The Chemistry of the Superheavy Elements. I. Pseudopotentials for 111 and 112 and Relativistic Coupled Cluster Calculations for (112)H+, (112)F2, and (112)F4. *J. Chem. Phys.* **1997**, *106* (9), 3623–3632. https://doi.org/10.1063/1.473437.

(6) Yakushev, A. B.; Buklanov, G. V.; Chelnokov, M. L.; Chepigin, V. I.; Dmitriev, S. N.; Gorshkov, V. A.; Hübener, S.; Lebedev, V. Ya.; Malyshev, O. N.; Oganessian, Yu. Ts. First Attempt to Chemically Identify Element 112. *Radiochim. Acta* **2001**, *89* (11–12), 743–745. https://doi.org/10.1524/ract.2001.89.11-12.743.

(7) Pershina, V.; Bastug, T.; Jacob, T.; Fricke, B.; Varga, S. Intermetallic Compounds of the Heaviest Elements: The Electronic Structure and Bonding of Dimers of Element 112 and Its Homolog Hg. *Chem. Phys. Lett.* **2002**, *365* (1), 176–183. https://doi.org/10.1016/S0009-2614(02)01428-8.

(8) Pershina, V.; Bastug, T. Relativistic Effects on Experimentally Studied Gas-Phase Properties of the Heaviest Elements. *Chem. Phys.* **2005**, *311* (1), 139–150. https://doi.org/10.1016/j.chemphys.2004.09.030.
(9) Sarpe-Tudoran, C.; Fricke, B.; Anton, J.; Persina, V. Adsorption of Superheavy Elements on Metal Surfaces. *J. Chem. Phys.* **2007**, *126* (17), 174702. https://doi.org/10.1063/1.2727447.
(10) Mewes, J.-M.; Smits, O. R.; Kresse, G.; Schwerdtfeger, P. Copernicium: A Relativistic Noble Liquid. *Angew. Chem. Int. Ed.* **2019**, *58* (50), 17964–17968. https://doi.org/10.1002/anie.201906966.
(11) Yakushev, A. B.; Zvara, I.; Oganessian, Yu. Ts.; Belozerov, A. V.; Dmitriev, S. N.; Eichler, B.; Hübener, S.; Sokol, E. A.; Türler, A.; Yeremin, A. V.; Buklanov, G. V.; Chelnokov, M. L.; Chepigin, V. I.; Gorshkov, V. A.; Gulyaev, A. V.; Lebedev, V. Ya.; Malyshev, O. N.; Popeko, A. G.; Soverna, S.; Szeglowski, Z.; Timokhin, S. N.; Tretyakova, S. P.; Vasko, V. M.; Itkis, M. G. Chemical Identification and Properties of Element 112. *Radiochim. Acta* **2003**, *91* (8), 433–440. https://doi.org/10.1524/ract.91.8.433.20010.
(12) Gäggeler, H. W.; Brüchle, W.; Düllmann, C. E.; Dressler, R.; Eberhardt, K.; Eichler, B.; Eichler, R.; Folden, C. M.; Ginter, T. N.; Glaus, F.; Gregorich, K. E.; Haenssler, F.; Hoffman, D. C.; Jäger, E.; Jost, D. T.; Kirbach, U. W.; Kratz, J. V.; Nitsche, H.; Patin, J. B.; Pershina, V.; Piguet, D.; Qin, Z.; Rieth, U.; Schädel, M.; Schimpf, E.; Schausten, B.; Soverna, S.; Sudowe, R.; Thörle-Pospiech, P.; Trautmann, N.; Türler, A.; Vahle, A.; Wilk, P. A.; Wirth, G.; Yakushev, A. B.; von Zweidorf, A. Chemical and Nuclear Studies of Hassium and Element 112. *Nucl. Phys. A* **2004**, *734*, 208–212. https://doi.org/10.1016/j.nuclphysa.2004.01.036.
(13) Eichler, R.; Aksenov, N. V.; Belozerov, A. V.; Bozhikov, G. A.; Chepigin, V. I.; Dmitriev, S. N.; Dressler, R.; Gäggeler, H. W.; Gorshkov, V. A.; Haenssler, F.; Itkis, M. G.; Laube, A.; Lebedev, V. Ya.; Malyshev, O. N.; Oganessian, Yu. Ts.; Petrushkin, O. V.; Piguet, D.; Rasmussen, P.; Shishkin, S. V.; Shutov, A. V.; Svirikhin, A. I.; Tereshatov, E. E.; Vostokin, G. K.; Wegrzecki, M.; Yeremin, A. V. Chemical Characterization of Element 112. *Nature* **2007**, *447* (7140), 72–75. https://doi.org/10.1038/nature05761.
(14) Ferrier, M. G.; Kmak, K. N.; Kerlin, W. M.; Valdez, C. A.; Despotopulos, J. D. Transactinides Studies with Sulfur Macrocyclic Extractant Using Mercury. *J. Radioanal. Nucl. Chem.* **2020**, *326*, 215–222.
(15) Tsuchiya, T.; Shimizu, T.; Kamigata, N. Unsaturated Thiacrown Ethers: Synthesis, Physical Properties, and Formation of a Silver Complex. *J. Am. Chem. Soc.* **2001**, *123* (47), 11534–11538. https://doi.org/10.1021/ja0102742.
(16) Tsuchiya, T.; Shimizu, T.; Hirabayashi, K.; Kamigata, N. Formation and Structures of Mercury Complexes of 18-Membered Unsaturated and Saturated Thiacrown Ethers. *J. Org. Chem.* **2003**, *68* (9), 3480–3485. https://doi.org/10.1021/jo020668r.
(17) Sun, D.-Q.; Yang, J.-K. An Economical Approach to the Synthesis of Unsaturated Thiacrown Ethers. *Synthesis* **2011**, *2011* (15), 2454–2458. https://doi.org/10.1055/s-0030-1260066.
(18) Despotopulos, J. D.; Kmak, K. N.; Shaughnessy, D. A. Production and Isolation of ^{197m,g}Hg. *J. Radioanal. Nucl. Chem.* **2018**, *317* (2), 985–989. https://doi.org/10.1007/s10967-018-5927-9.

(19) te Velde, G.; Bickelhaupt, F. M.; Baerends, E. J.; Fonseca Guerra, C.; van Gisbergen, S. J. A.; Snijders, J. G.; Ziegler, T. Chemistry with ADF. *J. Comput. Chem.* **2001**, *22* (9), 931–967. https://doi.org/10.1002/jcc.1056.
(20) Van Lenthe, E.; Baerends, E. J.; Snijders, J. G. Relativistic Regular Two-component Hamiltonians. *J. Chem. Phys.* **1993**, *99* (6), 4597–4610. https://doi.org/10.1063/1.466059.
(21) Zhang, Y.; Yang, W. Comment on "Generalized Gradient Approximation Made Simple." *Phys Rev Lett* **1998**, *80* (4), 890–890. https://doi.org/10.1103/PhysRevLett.80.890.
(22) Perdew, J. P.; Burke, K.; Ernzerhof, M. Generalized Gradient Approximation Made Simple. *Phys Rev Lett* **1996**, *77* (18), 3865–3868. https://doi.org/10.1103/PhysRevLett.77.3865.
(23) Hammer, B.; Hansen, L. B.; Nørskov, J. K. Improved Adsorption Energetics within Density-Functional Theory Using Revised Perdew-Burke-Ernzerhof Functionals. *Phys Rev B* **1999**, *59* (11), 7413–7421. https://doi.org/10.1103/PhysRevB.59.7413.
(24) Grimme, S.; Antony, J.; Ehrlich, S.; Krieg, H. A Consistent and Accurate Ab Initio Parametrization of Density Functional Dispersion Correction (DFT-D) for the 94 Elements H-Pu. *J. Chem. Phys.* **2010**, *132* (15), 154104. https://doi.org/10.1063/1.3382344.
(25) Grimme, S.; Ehrlich, S.; Goerigk, L. Effect of the Damping Function in Dispersion Corrected Density Functional Theory. *J. Comput. Chem.* **2011**, *32* (7), 1456–1465. https://doi.org/10.1002/jcc.21759.
(26) Van Lenthe, E.; Baerends, E. J. Optimized Slater-Type Basis Sets for the Elements 1–118. *J. Comput. Chem.* **2003**, *24* (9), 1142–1156. https://doi.org/10.1002/jcc.10255.
(27) Trombach, L.; Ehlert, S.; Grimme, S.; Schwerdtfeger, P.; Mewes, J.-M. Exploring the Chemical Nature of Super-Heavy Main-Group Elements by Means of Efficient Plane-Wave Density-Functional Theory. *Phys. Chem. Chem. Phys.* **2019**, *21* (33), 18048–18058. https://doi.org/10.1039/C9CP02455G.
(28) Harder, E.; Damm, W.; Maple, J.; Wu, C.; Reboul, M.; Xiang, J. Y.; Wang, L.; Lupyan, D.; Dahlgren, M. K.; Knight, J. L.; Kaus, J. W.; Cerutti, D. S.; Krilov, G.; Jorgensen, W. L.; Abel, R.; Friesner, R. A. OPLS3: A Force Field Providing Broad Coverage of Drug-like Small Molecules and Proteins. *J. Chem. Theory Comput.* **2016**, *12* (1), 281–296. https://doi.org/10.1021/acs.jctc.5b00864.
(29) Klamt, A.; Schüürmann, G. COSMO: A New Approach to Dielectric Screening in Solvents with Explicit Expressions for the Screening Energy and Its Gradient. *J. Chem. Soc. Perkin Trans. 2* **1993**, No. 5, 799–805. https://doi.org/10.1039/P29930000799.
(30) Pye, C. C.; Ziegler, T. An Implementation of the Conductor-like Screening Model of Solvation within the Amsterdam Density Functional Package. *Theor. Chem. Acc.* **1999**, *101* (6), 396–408. https://doi.org/10.1007/s002140050457.
(31) Powell Kipton J.; Brown Paul L.; Byrne Robert H.; Gajda Tamás; Hefter Glenn; Sjöberg Staffan; Wanner Hans. Chemical Speciation of Environmentally Significant Heavy Metals With Inorganic Ligands. Part 1: The Hg2+– Cl–, OH–, CO3 2–, SO4 2–, and PO4 3– Aqueous Systems. *Pure Appl. Chem.* **2005**, *7* (4), 739–800. https://doi.org/10.1351/pac200577040739.
(32) Herbst, R. S.; Brewer, K. N.; Tranter, T. J.; Todd, T. A. Mercury Extraction by the TRUEX Process Solvent. I. Kinetics, Extractable Species, & Dependence on Nitric Acid Concentration. *Solvent Extr. Ion Exch.* **1995**, *13* (3), 431–446. https://doi.org/10.1080/07366299508918284.

(33) Sato, T.; Nakamura, T. The Stability Constants of the Aqueous Chloro Complexes of Divalent Zinc, Cadmium and Mercury Determined by Solvent Extraction with Tri-n-Octylphosphine Oxide. *Hydrometallurgy* **1980**, *6* (1), 3–12. https://doi.org/10.1016/0304-386X(80)90003-1.
(34) Roesmer, J.; Kruger, P. *The Radiochemistry of Mercury*; Nuclear Science Series; Technical Report NAS-NS-3026(Rev); United States, 1970; p 211.
(35) Sevdić, D.; Fekete, L.; Meider, H. Macrocyclic Polythiaethers as Solvent Extraction Reagents—III: Extraction and Complex Formation of Silver(I) and Mercury(II) Picrates. *J. Inorg. Nucl. Chem.* **1980**, *42* (6), 885–889. https://doi.org/10.1016/0022-1902(80)80462-3.
(36) Sevdić, D.; Meider, H. Macrocyclic Polythiaethers as Solvent Extraction Reagents—IV Ag(I) and Hg(II) Complexes with 1,4,7,10,13,16-Hexathiacyclooctadecane. *J. Inorg. Nucl. Chem.* **1981**, *43* (1), 153–157. https://doi.org/10.1016/0022-1902(81)80452-6.
(37) Herceg, M.; Matković-Čalogović, D. Tetrabromo(1,4,7,10,13,16-Hexathiacyclooctadecane)Dimercury(II). *Acta Crystallogr. Sect. C* **1992**, *48* (10), 1779–1782. https://doi.org/10.1107/S0108270192002671.
(38) Ghosh, A.; Conradie, J. The Valence States of Copernicium and Flerovium. *Eur. J. Inorg. Chem.* **2016**, *2016* (18), 2989–2992. https://doi.org/10.1002/ejic.201600146.
(39) Baumann, T. F.; Reynolds, J. G.; Fox, G. A. Polymer Pendant Crown Thioethers: Synthesis and HgII Extraction Studies of a Novel Thiacrown Polymer. *Chem Commun* **1998**, No. 16, 1637–1638. https://doi.org/10.1039/A803383H.
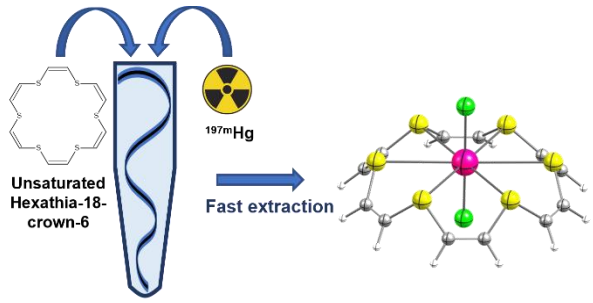
SYNOPSIS: The extraction of Hg(II) homolog to the superheavy element Cn(II) was investigated with UHT18C6. Computational study was performed to understand the bonding between Hg(II) and UHT18C6, as well as to predict the stability of the Cn(II):UHT18C6 complex.